



Fermi National Accelerator Laboratory

FERMILAB-Pub-98/342-T

**Trilepton Signature of Minimal Supergravity at the Upgraded
Tevatron**

V. Barger and C. Kao

*Fermi National Accelerator Laboratory
P.O. Box 500, Batavia, Illinois 60510*

December 1998

Submitted to *Physical Review D*

Disclaimer

This report was prepared as an account of work sponsored by an agency of the United States Government. Neither the United States Government nor any agency thereof, nor any of their employees, makes any warranty, expressed or implied, or assumes any legal liability or responsibility for the accuracy, completeness, or usefulness of any information, apparatus, product, or process disclosed, or represents that its use would not infringe privately owned rights. Reference herein to any specific commercial product, process, or service by trade name, trademark, manufacturer, or otherwise, does not necessarily constitute or imply its endorsement, recommendation, or favoring by the United States Government or any agency thereof. The views and opinions of authors expressed herein do not necessarily state or reflect those of the United States Government or any agency thereof.

Distribution

Approved for public release; further dissemination unlimited.

Copyright Notification

This manuscript has been authored by Universities Research Association, Inc. under contract No. DE-AC02-76CHO3000 with the U.S. Department of Energy. The United States Government and the publisher, by accepting the article for publication, acknowledges that the United States Government retains a nonexclusive, paid-up, irrevocable, worldwide license to publish or reproduce the published form of this manuscript, or allow others to do so, for United States Government Purposes.

Trilepton Signature of Minimal Supergravity at the Upgraded Tevatron

V. Barger^{1,2} and Chung Kao²

¹*Fermi National Accelerator Laboratory, P.O. Box 500, Batavia, IL 60510*

²*Department of Physics, University of Wisconsin, Madison, WI 53706*

Abstract

The prospects for detecting trilepton events ($\ell = e$ or μ) from chargino-neutralino ($\chi_1^\pm \chi_2^0$) associated production are investigated for Run II and Run III at the Fermilab Tevatron Collider in the context of the minimal supergravity model (mSUGRA). In some regions of parameter space, χ_1^\pm and χ_2^0 decay dominantly into final states with τ leptons and the contributions from τ -leptonic decays enhance the trilepton signal substantially when soft cuts on lepton transverse momenta are used. The dilepton (l^+l^-) invariant mass distribution near the endpoint is considered as a test of mSUGRA mass relations for a case with a large trilepton signal. Additional sources of the mSUGRA trilepton signal are discussed. Discovery contours for $p\bar{p} \rightarrow 3\ell + X$ at 2 TeV with an integrated luminosity of 2 fb^{-1} to 30 fb^{-1} are presented in the mSUGRA parameter space of $(m_{1/2}, m_0)$ for several choices of $\tan \beta$.

I. INTRODUCTION

In the near future the Main Injector (MI) of the Fermilab Tevatron Collider will run at 2 TeV center of mass energy and accumulate an integrated luminosity (L) of 2 fb^{-1} (Run II) or more at each of the CDF and the $D\bar{0}$ detectors. It has been proposed to further upgrade the Tevatron luminosity to $10^{33} \text{ cm}^{-2} \text{ s}^{-1}$ (Run III) to obtain an integrated luminosity $L = 30 \text{ fb}^{-1}$ [1,2]. Another possibility is to simply run with the MI for more years to accumulate a higher integrated luminosity. The order of magnitude increase in luminosity beyond the 0.1 fb^{-1} [3,4] now available will significantly improve the possibility that new physics beyond the Standard Model (SM) could be discovered before the CERN Large Hadron Collider (LHC) begins operation [2].

In this article we extend our recent study [5] on the prospects of detecting the trilepton signal with missing transverse energy in the minimal supergravity model (mSUGRA) at the upgraded Tevatron with a detailed consideration of suitable cuts to improve the trilepton search. The primary source of trileptons is associated production of the lighter chargino (χ_1^\pm) and the second lightest neutralino (χ_2^0) with both decaying to leptons [6,7]. In mSUGRA with gauge coupling unification, the sleptons ($\tilde{\ell}$), the lighter chargino (χ_1^\pm) and the lighter neutralinos (χ_1^0, χ_2^0) are considerably less massive than the gluinos and squarks over most of the parameter space. Because of this, the trilepton signal ($3\ell + \cancel{E}_T$) is one of the most promising channels [3,4,6,7] for supersymmetric particle searches at the Tevatron. The background from SM processes can be greatly reduced with suitable cuts.

A supersymmetry (SUSY) between fermions and bosons provides a natural explanation of the Higgs mechanism for electroweak symmetry breaking (EWSB) in the framework of a grand unified theory (GUT). For the particle content of the minimal supersymmetric standard model (MSSM) [8], the evolution of gauge couplings by renormalization group equations (RGEs) [9] is consistent with a grand unified scale at $M_{\text{GUT}} \sim 2 \times 10^{16} \text{ GeV}$ and an effective SUSY mass scale in the range $M_Z < M_{\text{SUSY}} \lesssim 10 \text{ TeV}$ [10]. With a large top quark Yukawa coupling (Y_t) to a Higgs boson at the GUT scale, radiative corrections drive

the corresponding Higgs boson mass squared parameter negative, spontaneously breaking the electroweak symmetry and naturally explaining the origin of the electroweak scale.

In SUGRA models [11], supersymmetry is broken in a hidden sector with SUSY breaking communicated to the observable sector through gravitational interactions, leading naturally but not necessarily [12] to a common scalar mass (m_0), a common gaugino mass ($m_{1/2}$), a common trilinear coupling (A_0) and a common bilinear coupling (B_0) at the GUT scale. Through minimization of the Higgs potential, the B coupling parameter of the superpotential and the magnitude of the Higgs mixing parameter μ are related to the ratio of Higgs-field vacuum expectation values (VEVs) ($\tan\beta \equiv v_2/v_1$) and to the mass of the Z boson (M_Z). The SUSY particle masses and couplings at the weak scale can be predicted by the evolution of RGEs from the unification scale [13,14]. In our analysis we assume universal boundary conditions at M_{GUT} with a common gaugino mass $m_{1/2}$ and a common scalar mass m_0 to study the production cross section and decay branching fractions of χ_1^\pm and χ_2^0 . Non-universal boundary conditions among sfermion masses can make $m_{\tilde{\tau}}$ larger than $m_{\tilde{\ell}}(\ell = e, \mu)$. For $m_{1/2} = 200$ GeV and $\tan\beta \lesssim 25$, this non-universality significantly enhances the trilepton signal when 50 GeV $\lesssim m_0 \lesssim 130$ GeV [15].

We evaluate SUSY mass spectra and couplings in the minimal supergravity model in terms of four parameters: m_0 , $m_{1/2}$, A_0 and $\tan\beta$, along with the sign of the Higgs mixing parameter μ . The value of A_0 does not significantly affect our analysis, therefore, we take $A_0 = 0$ in our calculations. The mass matrix of the charginos in the basis of the weak eigenstates ($\tilde{W}^\pm, \tilde{H}^\pm$) has the following form

$$M_C = \begin{pmatrix} M_2 & \sqrt{2}M_W \sin\beta \\ \sqrt{2}M_W \cos\beta & \mu \end{pmatrix}. \quad (1)$$

Since this mass matrix is not symmetric, its diagonalization requires two matrices [8]. The sign of the μ contribution in Eq. (1) establishes our sign convention for μ , which is equivalent to the ISAJET convention [16].

In Figure 1, we present the masses of the lightest neutralino (χ_1^0), the second lightest

neutralino (χ_2^0), the lighter chargino χ_1^\pm , the scalar electrons \tilde{e}_L and \tilde{e}_R , the lighter tau slepton ($\tilde{\tau}_1$), and the lighter bottom squark \tilde{b}_1 at the mass scale of M_Z , and the mass of the lighter CP-even Higgs scalar (h^0) at the scale $Q = \sqrt{m_{\tilde{t}_L} m_{\tilde{t}_R}}$ [17,18], versus m_0 , with $M_{\text{SUSY}} = 1$ TeV, $m_{1/2} = 200$ GeV and $\mu > 0$ for (a) $\tan\beta = 2$ and (b) $\tan\beta = 35$. To a good approximation, the mass of the lightest chargino $m_{\chi_1^\pm} \sim m_{\chi_2^0}$ is about twice $m_{\chi_1^0}$. Also shown in Fig. 1 are the regions that do not satisfy the following theoretical requirements: electroweak symmetry breaking (EWSB), tachyon free, and the lightest neutralino as the lightest SUSY particle (LSP). The region excluded by the $m_{\chi_1^\pm} \lesssim 90$ GeV limit from the chargino search [19,20] at LEP 2 is indicated. There are several interesting aspects to note in Fig. 1:

- (i) An increase in $\tan\beta$ leads to a larger m_h but a slight reduction in $m_{\chi_1^0}$, $m_{\chi_1^\pm}$, and a large reduction of $m_{\tilde{\tau}_1}$ and $m_{\tilde{b}_1}$.
- (ii) Increasing m_0 raises the masses of scalar fermions significantly.
- (iii) In most of the mSUGRA parameter space, the weak-scale gaugino masses are related to the universal gaugino mass parameter $m_{1/2}$ by

$$\begin{aligned}
m_{\chi_1^0} &\sim 0.44m_{1/2}, \quad \text{and} \\
m_{\chi_1^\pm} &\sim m_{\chi_2^0} \sim 0.84m_{1/2}.
\end{aligned}
\tag{2}$$

Consequently, the trilepton channel could provide valuable information about the value of $m_{1/2}$.

The masses of χ_1^\pm and χ_2^0 to the leading order in $M_W^2/(\mu^2 - M_2^2)$ can be expressed as [21]

$$\begin{aligned}
m_{\chi_1^\pm} &= M_2 - \frac{M_W^2 (M_2 + \mu \sin 2\beta)}{\mu^2 - M_2^2 + 2M_W^2}, \\
m_{\chi_2^0} &= M_2 - \frac{M_W^2 (M_2 + \mu \sin 2\beta)}{\mu^2 - M_2^2}
\end{aligned}
\tag{3}$$

We find that M_2 and $|\mu|$ can be empirically expressed in GeV units as a function of the GUT scale masses $m_{1/2}$, m_0 and $\cos 2\beta$ as

$$M_2 = 0.851m_{1/2} + 0.00244m_0 - 2.20,$$

$$\begin{aligned}
|\mu| &= am_{1/2} + b \cos 2\beta + c, \\
a &= 2.34 - 0.153(m_0/100 \text{ GeV}) + [1.10 - 0.141(m_0/100 \text{ GeV})] \cos 2\beta, \\
b &= 1.787m_0 - 167.5, \\
c &= 1.909m_0 - 178.7.
\end{aligned}
\tag{4}$$

for $100 \text{ GeV} \lesssim m_0, m_{1/2} \lesssim 1000 \text{ GeV}$ and all $\tan\beta$ for which perturbative RGE solutions exist. These mass formulas for M_2 , χ^\pm , χ_2^0 , and $|\mu|$ hold to an accuracy of $\lesssim 2\%$, 4% , 4% , and 8% , respectively.

The Yukawa couplings of the bottom quark (b) and the tau lepton (τ) are proportional to $\tan\beta$ and are thus greatly enhanced when $\tan\beta$ is large. In SUSY GUTS, the masses of the third generation sfermions are consequently very sensitive to the value of $\tan\beta$. As $\tan\beta$ increases, the lighter tau slepton ($\tilde{\tau}_1$) and the lighter bottom squark (\tilde{b}_1) become lighter than charginos and neutralinos while other sleptons and squarks remain heavy. Then, χ_1^\pm and χ_2^0 can dominantly decay into final states with tau leptons via real or virtual $\tilde{\tau}_1$. While the contributions from these decays reduce the trilepton signal when hard cuts are used to suppress the backgrounds [7,23], they also open new discovery channels via the soft leptons from τ decays [5].

One way to detect τ leptons is through their one prong and three prong hadronic decays. The CDF and the D0 collaborations are currently investigating the efficiencies for detecting these modes and for implementing a τ trigger [22]. It has been suggested that the τ leptons in the final state may be a promising way to search for $\chi_1^\pm\chi_2^0$ production at the Tevatron if excellent τ identification becomes feasible [23–25].

Another way of exploiting the τ signals, that we consider in this article, is to include the soft electrons and muons from leptonic τ decays by employing softer but realistic p_T cuts on the leptons than conventionally used [7]. We find that this can significantly improve the trilepton signal from $\chi_1^\pm\chi_2^0$ production [5].

Recent measurements of the $b \rightarrow s\gamma$ decay rate by the CLEO [26] and LEP collaborations [27] place constraints on the parameter space of the minimal supergravity model [28]. It was

found that $b \rightarrow s\gamma$ excludes most of the minimal supergravity (mSUGRA) parameter space when $\tan\beta$ is large ($\tan\beta \gtrsim 10$) and $\mu < 0$ [28]. Therefore, we consider only $\mu > 0$ in our analysis when $\tan\beta \geq 10$.

In section II we discuss the $p\bar{p} \rightarrow \chi_1^\pm \chi_2^0 + X$ cross section and the decay branching fractions of χ_1^\pm and χ_2^0 . The acceptance cuts for the signal and background are discussed in Section III. We present trilepton cross section from additional SUSY sources in Section IV. When the sleptons ($\tilde{\ell}$) and the sneutrinos ($\tilde{\nu}$) are light, they also contribute to the trilepton signal via production of $\tilde{\ell}\tilde{\ell}$ and $\tilde{\ell}\tilde{\nu}$. These contributions are at interesting levels when $m_0 \lesssim 150$ GeV and $\tan\beta \gtrsim 20$. The discovery potential of the trilepton search at the upgraded Tevatron is presented in Section V, with 3σ significance contours for observation or exclusion and 5σ significance contours for discovery. Section VI discusses the end point reconstruction at the Run III for invariant mass distribution of l^+l^- from the χ_2^0 decays. Our conclusions are given in Section VII.

II. ASSOCIATED PRODUCTION OF CHARGINO AND NEUTRALINO

In hadron collisions the associated production of the lighter chargino and the second lightest neutralino occurs via quark-antiquark annihilation in the s -channel through a virtual W boson ($q\bar{q}' \rightarrow W^{\pm*} \rightarrow \chi_1^\pm \chi_2^0$) and in the t and u -channels through squark (\tilde{q}) exchanges. Figure 2 shows the Feynman diagrams of $q\bar{q}' \rightarrow \chi_1^\pm \chi_2^0$. The $p\bar{p} \rightarrow \chi_1^\pm \chi_2^0 + X$ cross section depends mainly on masses of the chargino ($m_{\chi_1^\pm}$) and the neutralino ($m_{\chi_2^0}$). For squarks much heavier than the gauginos, the s -channel W -resonance amplitude dominates. If the squarks are light, a destructive interference between the W boson and the squark exchange amplitudes can suppress the cross section by as much as 40% compared to the s -channel contribution alone. For larger squark masses, the effect of negative interference is reduced.

Feynman diagrams of the chargino and neutralino decays into final states of leptons and neutrinos and the LSP are shown in Figure 3: (a) $\chi_1^\pm \rightarrow \ell\nu\chi_1^0$ or $\tau\nu\chi_1^0$ and (b) $\chi_2^0 \rightarrow \ell^+\ell^-\chi_1^0$ or $\tau^+\tau^-\chi_1^0$. Figure 4 presents the branching fractions of χ_2^0 versus $\tan\beta$, with

$m_{1/2} = 200$ GeV and several values of m_0 for both $\mu > 0$ and $\mu < 0$. For $\tan \beta \lesssim 5$, the branching fractions are sensitive to the sign of μ .

For $\mu > 0$, and $\tan \beta \sim 2$, we observe that the dominant decays are:

$$\begin{aligned}
m_0 \lesssim 50 \text{ GeV:} & \quad \chi_1^\pm \rightarrow \tilde{\nu}_L \ell \text{ and } \tilde{\tau}_1 \nu, \\
& \quad \chi_2^0 \rightarrow \tilde{\ell}_R \ell, \tilde{\tau}_1 \tau \text{ and } \tilde{\nu}_L \nu; \\
60 \text{ GeV} \lesssim m_0 \lesssim 110 \text{ GeV:} & \quad \chi_1^\pm \rightarrow \tilde{\tau}_1 \nu, \\
& \quad \chi_2^0 \rightarrow \tilde{\ell}_R \ell \text{ and } \tilde{\tau}_1 \tau, (\chi_2^0 \rightarrow \tilde{\nu}_L \nu \text{ suppressed}); \\
120 \text{ GeV} \lesssim m_0 \lesssim 170 \text{ GeV:} & \quad \chi_1^\pm \chi_2^0 \rightarrow 3\ell + \cancel{E}_T \text{ via virtual } \tilde{\ell}; \\
m_0 \gtrsim 180 \text{ GeV:} & \quad \chi_1^\pm, \chi_2^0 \rightarrow q\bar{q}\chi_1^0.
\end{aligned}$$

For $\mu < 0$ and $\tan \beta \sim 2$, the dominant decays are:

$$\begin{aligned}
m_0 \lesssim 100 \text{ GeV:} & \quad \chi_1^\pm \rightarrow \tilde{\nu}_L \ell, \\
& \quad \chi_2^0 \rightarrow \tilde{\nu}_L \nu; \\
m_0 \gtrsim 110 \text{ GeV:} & \quad \chi_1^\pm \rightarrow \tilde{\tau}_1 \nu, \\
& \quad \chi_2^0 \rightarrow \chi_1^0 h^0.
\end{aligned}$$

For $m_0 \sim 200$ GeV, χ_2^0 dominantly decays (i) into $\tau\bar{\tau}\chi_1^0$ for $25 \lesssim \tan \beta \lesssim 40$, (ii) into $\tau\tilde{\tau}_1$ for $\tan \beta \gtrsim 40$. For $m_0 \lesssim 300$ GeV and large $\tan \beta \gtrsim 35$, both $\tilde{\tau}_1$ and \tilde{b}_1 can be lighter than other sfermions, and χ_1^\pm and χ_2^0 can decay dominantly into final states with τ leptons or b quarks via virtual or real $\tilde{\tau}_1$ and \tilde{b}_1 . For $m_0 \gtrsim 400$ GeV and $5 \lesssim \tan \beta \lesssim 40$, $B(\chi_2^0 \rightarrow \tau^+\tau^-\chi_1^0) \sim B(\chi_2^0 \rightarrow e^+e^-\chi_1^0) \sim 2\%$

Figure 5 shows the cross section $\sigma(p\bar{p} \rightarrow \chi_1^\pm \chi_2^0 \rightarrow 3\ell + X)$ at $\sqrt{s} = 2$ TeV, which is the product $\sigma(p\bar{p} \rightarrow \chi_1^\pm \chi_2^0 + X) \times B(\chi_1^\pm \rightarrow \ell\nu\chi_1^0) \times B(\chi_2^0 \rightarrow \ell^+\ell^-\chi_1^0)$, versus $\tan \beta$ without acceptance cuts, with $m_{1/2} = 200$ GeV and several values of m_0 for both $\mu > 0$ and $\mu < 0$. For $\tan \beta \lesssim 5$, the branching fractions are sensitive to the sign of μ . For $\mu < 0$ and $\tan \beta \sim 2$, (a) with $m_0 = 100$ GeV, $B(\chi_2^0 \rightarrow \tilde{\nu}\nu) = 0.71$ and $B(\chi_2^0 \rightarrow h^0\chi_1^0) = 0.19$, some trileptons are due to $\chi_2^0 \rightarrow \tilde{\ell}_R \ell$ and $\tilde{\tau}_1 \tau$. (b) with $m_0 = 200$ GeV, $B(\chi_2^0 \rightarrow h^0\chi_1^0) = 0.99$ and consequently the trilepton rate drops sharply.

III. ACCEPTANCE CUTS

In this section we present results from simulations with an event generator and a simple calorimeter including our acceptance cuts. The ISAJET 7.40 event generator program [16] is employed to calculate the $3\ell + \cancel{E}_T$ signal from $\chi_1^\pm \chi_2^0$ and the dominant backgrounds from WZ and $t\bar{t}$ at the upgraded Tevatron. A calorimeter with segmentation $\Delta\eta \times \Delta\phi = 0.1 \times (2\pi/24)$ extending to $|\eta| = 4$ is used. An energy resolution of $\frac{0.7}{\sqrt{E}}$ for the hadronic calorimeter and $\frac{0.15}{\sqrt{E}}$ for the electromagnetic calorimeter is assumed. Jets are defined to be hadron clusters with $E_T > 15$ GeV in a cone with $\Delta R = \sqrt{\Delta\eta^2 + \Delta\phi^2} = 0.7$. Leptons with $p_T > 5$ GeV and within $|\eta_\ell| < 2.0$ are considered to be isolated if the hadronic scalar E_T in a cone with $\Delta R = 0.4$ about the lepton is smaller than 2 GeV.

The trilepton signal from charginos and neutralinos at the Tevatron has dominant backgrounds come from WZ and $t\bar{t}$ production. Most backgrounds from the SM processes can be removed with the following three cuts:

1. We require that there must be 3 isolated leptons in each event¹ with $p_T > 5$ GeV and $|\eta_\ell| < 2.0$ and that the hadronic scalar E_T in a cone with $\Delta R = 0.4$ around the lepton should be smaller than 2 GeV. This isolation cut remove background from $b\bar{b}$ and $c\bar{c}$ decays.
2. We require $\cancel{E}_T > 25$ GeV in each event to remove backgrounds from SM processes such as Drell-Yan dilepton production, where an accompanying jet may fake a lepton.
3. To reduce the background from WZ production, we require that the invariant mass of any opposite-sign dilepton pair not reconstruct the Z mass: $|M(\ell^+\ell^-) - M_Z| \geq 10$ GeV. This cut reduces most of the WZ background.

The surviving total background after these two cuts is mainly due to WZ events, where $Z \rightarrow \tau\bar{\tau}$, with subsequent τ -leptonic decays.

¹The events with 4 isolated leptons are considered as the 4-lepton signals in our analysis.

Figure 6 presents the transverse momentum (p_T) distribution of the three leptons at $\sqrt{s} = 2$ TeV, for $p\bar{p} \rightarrow 3\ell + X$ with $\mu > 0$, $\tan\beta = 10$, $m_{1/2} = 200$ GeV and $m_0 = 100$ GeV. The p_T distribution for the dominant background from $p\bar{p} \rightarrow W^\pm Z \rightarrow 3\ell + X$ via $Z \rightarrow \tau^+\tau^- \rightarrow l^+l^- + X$ is shown in Figure 7. We label the trileptons as $\ell_{1,2,3}$, where $\ell = e$ or μ , according to the ordering $p_T(\ell_1) > p_T(\ell_2) > p_T(\ell_3)$ of their transverse momenta. The most important lesson that we learn from Fig. 6 and Fig. 7 is that most ℓ_3 's from the $\chi^\pm\chi_2^0$ decays have smaller p_T than the ℓ_3 's from $W^\pm Z$ decays. Therefore, it is very important to have a soft acceptance cut on $p_T(\ell_3)$ to retain the trilepton events from $\chi_1^\pm\chi_2^0$ decays.

Our acceptance cuts are chosen to be consistent with the experimental cuts proposed for Run II [29] at the Tevatron as follows:

$$\begin{aligned}
& p_T(\ell_1) > 11 \text{ GeV}, \quad p_T(\ell_2) > 7 \text{ GeV}, \quad p_T(\ell_3) > 5 \text{ GeV}, \\
& |\eta(\ell_1, \ell_2, \ell_3)| < 2.0, \\
& \text{at least one } \ell \text{ with } p_T(\ell) > 11 \text{ GeV}, \quad \text{and } |\eta(\ell)| < 1.0, \\
& \cancel{E}_T > 25 \text{ GeV}, \\
& |M(\ell\bar{\ell}) - M_Z| \geq 10 \text{ GeV}. \tag{5}
\end{aligned}$$

The surviving total background cross section from WZ , $t\bar{t}$ and ZZ is about 0.58 fb. This residual background is mainly due to WZ production with $Z \rightarrow \tau\bar{\tau}$ and subsequent τ leptonic decays. The \cancel{E}_T cut removes backgrounds from Drell-Yan dilepton production, where an accompanying jet may fake a lepton. Our background cross sections from WZ and ZZ are in good agreement with the CDF Run II studies [30]. The $t\bar{t}$ background in our analysis is larger than that found in Ref. [30]. This difference in the $t\bar{t}$ background calculations suggests that the CDF detector simulations are more efficient in making isolation cuts than the ISAJET calorimeter.

The effect of cuts on the signal and background is demonstrated in Table I. The trileptons are due to $\chi_1^\pm\chi_2^0$ production and the additional SUSY particle sources that are discussed in the next section. The cross sections of the signal with $m_{1/2} = 200$ GeV, $m_0 = 100$ GeV, and several values of $\tan\beta$, along with WZ , $t\bar{t}$ and ZZ backgrounds are presented for four

cases: (a) Soft Cuts, (b) Soft Cuts and Jet Veto; here we veto events with any jet that has $E_T > 15$ GeV, (c) Hard Cuts and (d) Hard Cuts and Jet Veto [7]. We note that (i) the soft cuts enhance the signal by about a factor of two for $3 \lesssim \tan \beta \lesssim 25$; (ii) the inclusive trilepton signal cross section is about twice that of the clean trilepton signal without jets.

At Run II with 2 fb^{-1} integrated luminosity, we expect about one event per experiment from the background cross section of 0.58 fb . The signal cross section must yield a minimum of four signal events for discovery. The Poisson probability for the SM background to fluctuate to this level is less than 0.4% . At Run III with $L = 30 \text{ fb}^{-1}$, we would expect about 17 background events; a 5σ signal would be 21 events corresponding to a signal cross section of 0.70 fb , and a 3σ signal would be 12 events corresponding to a signal cross section of 0.42 fb .

IV. ADDITIONAL SOURCES OF TRILEPTONS

In addition to the associated production of $\chi_1^\pm \chi_2^0$, there are other SUSY contributions to the trilepton signature.

1. If the sleptons and sneutrinos are light, they can make important contribution to the trilepton signal from production of $\tilde{\ell}\tilde{\nu}$ and $\tilde{\ell}\tilde{\ell}$, along with a small contribution from $\tilde{\nu}\tilde{\nu}$.
2. When the charginos ($\chi_{1,2}^\pm$), and the neutralinos ($\chi_{2,3,4}^0$) are not too heavy, they contribute to the trilepton signal via $\chi_2^0\chi_2^0$, $\chi_2^0\chi_3^0$, $\chi_3^0\chi_4^0$, $\chi_1^\pm\chi_3^0$, $\chi_2^\pm\chi_3^0$, and $\chi_2^\pm\chi_4^0$ production.
3. When the gluino (\tilde{g}), the squarks (\tilde{q}), and the neutralinos ($\chi_{2,3,4}^0$) are not too heavy, they also contribute to the trilepton signal via the production of $\tilde{g}\chi_{2,3}^0$ and $\tilde{q}\chi_{2,3}^0$.
4. The production of $\tilde{g}\tilde{g}$ and $\tilde{q}\tilde{q}$ also make small contributions to trileptons.

For $m_0 \gtrsim 500$ GeV and $m_{1/2} \lesssim 300$ GeV, the associated production of $\chi_1^\pm \chi_2^0$, contributes at least 95% of the trilepton signal. For $m_0 \lesssim 150$ and $\tan \beta \gtrsim 20$, production of $\tilde{\ell}\tilde{\nu}$ and

$\tilde{\ell}\tilde{\ell}$ can enhance the trilepton cross section and may yield observable signals at Run III. We summarize the contributions to trileptons from various relevant channels for $\mu > 0$ in Table II and for $\mu < 0$ in Table III.

We separately consider the events with 4 isolated leptons. For $\tan\beta \lesssim 10$, $m_{1/2} \lesssim 200$ GeV, and $m_0 \lesssim 100$ GeV, the production of $p\bar{p} \rightarrow \chi_2^0\chi_2^0 \rightarrow 4\ell + X$ may be observable with an integrated luminosity $L \gtrsim 10 \text{ fb}^{-1}$. We apply the following acceptance cuts for the 4ℓ signal: (i) the hadronic scalar $E_T < 2.0$ GeV in a cone with $\Delta R = 0.4$, (ii) $p_T(\ell_1, \ell_2, \ell_3, \ell_4) > 11, 7, 5, 5$ GeV, (iii) $|\eta(\ell)| < 2.0$, (iv) at least one lepton with $p_T > 11$ GeV and $|\eta| < 1.0$, and (v) $\cancel{E}_T > 25$ GeV. The $p\bar{p} \rightarrow \chi_2^0\chi_2^0 \rightarrow 4\ell + X$ cross section after cuts is 0.79 fb and 0.24 fb for $\tan\beta = 3$ and 10, respectively, with $m_{1/2} = 200$ GeV and $m_0 = 100$ GeV. The cross section of the dominant background $p\bar{p} \rightarrow ZZ \rightarrow 4\ell + X$ is 0.17 fb. The cross sections of the 4ℓ signal with $m_{1/2} = 200$ GeV, $m_0 = 100$ GeV, and several values of $\tan\beta$, along with the ZZ background are presented in Table IV.

V. DISCOVERY POTENTIAL AT THE TEVATRON

The cross sections for the trilepton signal and the background after cuts are shown in Figure 8 versus $m_{1/2}$ with several values of m_0 for both $\mu > 0$ and $\mu < 0$ with $\tan\beta = 2$. With $L = 2 \text{ fb}^{-1}$ and $m_{1/2} = 200$ GeV, the trilepton signal may be observable for $m_0 \lesssim 350$ GeV and $m_0 \gtrsim 700$ GeV with $\mu > 0$ and for $m_0 \lesssim 150$ GeV with $\mu < 0$.

Figure 9 shows the cross sections of the trilepton signal and background after cuts versus $m_{1/2}$ with several values of m_0 , and $\mu > 0$ for $\tan\beta = 10$ and $\tan\beta = 35$. With $L = 2 \text{ fb}^{-1}$ and $m_{1/2} = 200$ GeV, the trilepton signal may be observable for $m_0 \lesssim 350$ GeV with $\tan\beta \sim 10$.

For $180 \text{ GeV} \lesssim m_0 \lesssim 400 \text{ GeV}$ and $10 \lesssim \tan\beta \lesssim 40$, the χ_2^0 decays dominantly into $q\bar{q}\chi_1^0$ and in these regions it will be difficult to establish a supersymmetry signal.

To assess the overall discovery potential of the upgraded Tevatron, we present the 99% C.L. (Run II) and 5σ (Run III) discovery contours and the 3σ observation contour for Run

III in Figure 10 for $p\bar{p} \rightarrow 3\ell + X$ at $\sqrt{s} = 2$ TeV, with soft acceptance cuts [Eq. (5)], in the parameter space of $(m_{1/2}, m_0)$, with $\tan\beta = 2$, for (a) $\mu > 0$ and (b) $\mu < 0$. We include all SUSY sources of trileptons for the signal. Also shown are the parts of the parameter space (i) excluded by theoretical requirements, or (ii) excluded by the chargino search at LEP 2. Figure 11 shows the 99% C.L. (Run II) and 5σ (Run III) discovery contours and the 3σ observation contour for Run III for $p\bar{p} \rightarrow 3\ell + X$ in the parameter space of $(m_{1/2}, m_0)$ for $\tan\beta = 10$ and $\tan\beta = 35$. All SUSY sources of trileptons are included.

We calculate cross sections for the signals and the backgrounds with tree level amplitudes. However, we expect that our conclusions and discovery contours will be valid after QCD radiative corrections are included. Recent studies found that QCD corrections enhance the signal cross section of $p\bar{p} \rightarrow \chi_1^\pm \chi_2^0 + X$ by about 10-30% for $300 \text{ GeV} \gtrsim m_{\chi_1^\pm} \gtrsim 70 \text{ GeV}$ [31]. QCD corrections also enhance the cross section of the dominant background $p\bar{p} \rightarrow W^\pm Z + X$ by about 30% [32].

VI. MASS RECONSTRUCTION

If the two-body decay $\chi_2^0 \rightarrow \tilde{\ell}_R \ell \rightarrow \ell^+ \ell^- + \chi_1^0$ is kinematically allowed, it may be possible to test a predicted mass relation [33–35] among $m_{\chi_2^0}$, $m_{\tilde{\ell}_R}$ and $m_{\chi_1^0}$, with a large integrated luminosity $L \sim 30 \text{ fb}^{-1}$. To demonstrate this interesting possibility, we consider the following parameters: $m_{1/2} = 200 \text{ GeV}$, $m_0 = 100 \text{ GeV}$, $A_0 = 0$, $\tan\beta = 3$ and $\mu > 0$. We evaluate masses and couplings of SUSY particles at the weak scale with renormalization group equations and obtain $m_{\chi_2^0} = 143 \text{ GeV}$, $m_{\tilde{\ell}_R} = 133 \text{ GeV}$, $m_{\chi_1^0} = 76.0$ and $\mu = 318$. The corresponding trilepton cross section after cuts $\sigma(p\bar{p} \rightarrow \chi_1^\pm \chi_2^0 \rightarrow 3\ell + \cancel{E}) = 11.1 \text{ fb}$, gives a promising signal with 333 events for $L = 30 \text{ fb}^{-1}$.

We consider the subtracted dilepton invariant mass distribution [33] defined as

$$\left. \frac{d\sigma}{dM} \right|_{\text{II}} = \left. \frac{d\sigma}{dM} \right|_{e^+e^-} + \left. \frac{d\sigma}{dM} \right|_{\mu^+\mu^-} - \left. \frac{d\sigma}{dM} \right|_{e^+\mu^-} - \left. \frac{d\sigma}{dM} \right|_{e^-\mu^+}. \quad (6)$$

The subtractions remove the lepton pairs with one lepton coming from χ_1^\pm and another

coming from χ_2^0 . This mass distribution has a sharp edge (endpoint) that appears near the kinematic limit for this decay sequence, i.e.,

$$M_{\ell\ell}^{\text{MAX}} = M_{\chi_2^0} \sqrt{1 - \frac{M_{\tilde{\ell}}^2}{M_{\chi_2^0}^2}} \sqrt{1 - \frac{M_{\chi_1^0}^2}{M_{\tilde{\ell}}^2}} \approx 45 \text{ GeV}. \quad (7)$$

Figure 12 shows the subtracted invariant mass distribution for two leptons with opposite signs (l^+l^-) from $p\bar{p} \rightarrow \chi_1^\pm \chi_2^0 \rightarrow 3\ell + X$ at $\sqrt{s} = 2$ TeV, with $\mu > 0$, $\tan\beta = 3$, $m_{1/2} = 200$ GeV, and $m_0 = 100$ GeV. This distribution may allow a test of the mSUGRA mass relations in this optimal case with a high cross section, provided that a large luminosity accumulation is obtained.

VII. CONCLUSIONS

In most of the mSUGRA parameter space, $\chi_1^\pm \chi_2^0$ production is the dominant source of trileptons. For $m_0 \lesssim 150$ and $\tan\beta \gtrsim 20$, production of $\tilde{\ell}\tilde{\nu}$ and $\tilde{\ell}\tilde{\ell}$ can enhance the trilepton signal and may yield observable rates at Run III in region of parameter space that are otherwise inaccessible.

In some regions of the mSUGRA parameter space, the χ_1^\pm and the χ_2^0 decay dominantly to final states with τ leptons. The subsequent leptonic decays of these τ leptons contribute importantly to the trilepton signal from $\chi_1^\pm \chi_2^0$ associated production. With soft but realistic lepton p_T acceptance cuts, these $\tau \rightarrow \ell$ contributions enhance the trilepton signal by at least a factor of two. The branching fractions of χ_1^\pm and χ_2^0 decays into τ leptons are dominant when the universal scalar mass m_0 is less than about 200 GeV and/or $\tan\beta \gtrsim 40$.

The Tevatron trilepton searches are most sensitive to the region of mSUGRA parameter space with $m_0 \lesssim 100$ GeV and $\tan\beta \lesssim 10$.

- For $m_0 \sim 100$ GeV and $\tan\beta \sim 3$, the trilepton signal should be detectable with 99% C.L. (i) at the MI if $m_{1/2} \lesssim 260$ GeV and (ii) at the Run III if $m_{1/2} \lesssim 290$ GeV.
- For $m_0 \sim 150$ GeV and $\tan\beta \sim 35$, the trilepton signal should be detectable at the Run III if $m_{1/2} \lesssim 170$ GeV.

- For $m_0 \gtrsim 500$ GeV and $\tan \beta \sim 35$, the trilepton signal should be detectable at the Run III if $m_{1/2} \lesssim 200$ GeV.

A difficult region for trileptons from $\chi_1^\pm \chi_2^0$ production is $180 \text{ GeV} \lesssim m_0 \lesssim 400 \text{ GeV}$ with $10 \lesssim \tan \beta \lesssim 35$, because for these parameters χ_1^\pm and χ_2^0 dominantly decay into $q\bar{q}'\chi_1^0$.

For $\tan \beta \lesssim 10$, $m_{1/2} \lesssim 200$ GeV, and $m_0 \lesssim 100$ GeV, the production of $p\bar{p} \rightarrow \chi_2^0 \chi_2^0 \rightarrow 4\ell + X$ at $\sqrt{s} = 2$ TeV may be observable with an integrated luminosity $L \gtrsim 10 \text{ fb}^{-1}$. The background from $p\bar{p} \rightarrow ZZ \rightarrow 4\ell + X$ is very small.

ACKNOWLEDGMENTS

VB thanks the Fermilab theory group for kind hospitality and support as a Frontier Fellow. We are grateful to Howie Baer, Regina Demina, Teruki Kamon, Wai-Yee Keung, Jane Nachtman, Frank Paige and Xerxes Tata for beneficial discussions. This research was supported in part by the U.S. Department of Energy under Grants No. DE-FG02-95ER40896 and in part by the University of Wisconsin Research Committee with funds granted by the Wisconsin Alumni Research Foundation.

REFERENCES

- [1] F.J. Gilman et al., *Planning for the Future of U.S. High-Energy Physics*, HEPAP Sub-panel Report, February, 1998.
- [2] D. Amidei and R. Brock et al., *Future Electroweak Physics at the Fermilab Tevatron*, Report of the TeV2000 Study Group, April 1996.
- [3] F. Abe et al., the CDF collaboration, *Phys. Rev. Lett.* **80**, 5275 (1998).
- [4] S. Abachi et al., the $D\bar{0}$ collaboration, *Phys. Rev. Lett.* **76** (1996) 4307.
- [5] V. Barger, C. Kao, T.-J. Li, *Phys. Lett. B* **433**, 328 (1998).
- [6] H. Baer, K. Hagiwara and X. Tata, *Phys. Rev. D***35**, 1598 (1987); R. Arnowitt and P. Nath, *Mod. Phys. Lett.* **A2**, 331 (1987); H. Baer and X. Tata, *Phys. Rev. D***47**, 2739 (1993); T. Kamon, J. Lopez, P. McIntyre and J. T. White, *Phys. Rev. D***50**, 5676 (1994); S. Mrenna, G. Kane, G. D. Kribs and J.D. Wells, *Phys. Rev. D***53**, 1168 (1996).
- [7] H. Baer, C. Kao and X. Tata *Phys. Rev. D***48** (1993) 5175; H. Baer, C.-H. Chen, C. Kao and X. Tata *Phys. Rev. D***52** (1995) 1565; H. Baer, C.-H. Chen, F. Paige and X. Tata, *Phys. Rev. D***54** (1996) 5866.
- [8] H.P. Nilles, *Phys. Rep.* **110** (1984) 1; H. Haber and G. Kane, *Phys. Rep.* **117** (1985) 75.
- [9] K. Inoue, A. Kakuto, H. Komatsu and H. Takeshita, *Prog. Theor. Phys.* **68** (1982) 927 and **71** (1984) 413.
- [10] P. Langacker and M. Luo, *Phys. Rev. D***44** (1991) 817; J. Ellis, S. Kelley and D. Nanopoulos, *Phys. Lett.* **B260** (1991) 131; U. Amaldi, W. de Boer and H. Fürstenau, *Phys. Lett.* **B260** (1991) 447; R. Barbieri, talk given at the 18th International Symposium on Lepton-Photon Interactions, Hamburg, Germany, July 1997, hep-ph/9711232.
- [11] A.H. Chamseddine, R. Arnowitt and P. Nath, *Phys. Rev. Lett.* **49** (1982) 970; L. Ibañez

- and G. Ross, Phys. Lett. **B110** (1982) 215; J. Ellis, D. Nanopoulos and K. Tamvakis, Phys. Lett. **B121** (1983) 123; L.J. Hall, J. Lykken and S. Weinberg, Phys. Rev. **D27** (1983) 2359; L. Alvarez-Gaumé, J. Polchinski and M. Wise, Nucl. Phys. **B121** (1983) 495.
- [12] V. Berezinskii et al., Astropart. Phys. **5** (1996) 1; P. Nath and R. Arnowitt, Phys. Rev. D **56**, 2820 (1997).
- [13] V. Barger, M.S. Berger, P. Ohmann, Phys. Rev. **D47** (1993) 1093; **D49** (1994) 4908; V. Barger, M.S. Berger, P. Ohmann and R.J.N. Phillips, Phys. Lett. **B314** (1993) 351.
- [14] J. Ellis and F. Zwirner, Nucl. Phys. **B338** (1990) 317; G. Ross and R.G. Roberts, Nucl. Phys. **B377** (1992) 571; R. Arnowitt and P. Nath, Phys. Rev. Lett. **69** (1992) 725; M. Drees and M.M. Nojiri, Nucl. Phys. **B369** (1993) 54; S. Kelley *et. al.*, Nucl. Phys. **B398** (1993) 3; M. Olechowski and S. Pokorski, Nucl. Phys. **B404** (1993) 590; G. Kane, C. Kolda, L. Roszkowski and J. Wells, Phys. Rev. **D49** (1994) 6173; D.J. Castaño, E. Piard and P. Ramond, Phys. Rev. **D49** (1994) 4882; W. de Boer, R. Ehret and D. Kazakov, Z. Phys. **67** (1995) 647; H. Baer, M. Drees, C. Kao, M. Nojiri and X. Tata, Phys. Rev. D **50** (1994) 2148; H. Baer, C.-H. Chen, R. Munroe, F. Paige and X. Tata, Phys. Rev. D **51** (1995) 1046.
- [15] E. Accomando, R. Arnowitt and B. Dutta, Texas A&M University Report CTP-TAMU-43-98 (1998), hep-ph/9811300.
- [16] F. Paige and S. Protopopescu, in *Supercollider Physics*, ed. D. Soper (World Scientific, 1986); H. Baer, F. Paige, S. Protopopescu and X. Tata, in *Proceedings of the Workshop on Physics at Current Accelerators and Supercolliders*, ed. J. Hewett, A. White and D. Zeppenfeld, (Argonne National Laboratory, 1993), hep-ph/9305342; *ISAJET 7.40: A Monte Carlo Event Generator for $pp, \bar{p}p$, and e^+e^- Reactions*, Brookhaven National Laboratory Report BNL-HET-98-39 (1998), hep-ph/9810440.

- [17] H. Baer, C.-H. Chen, M. Drees, F. Paige and X. Tata, Phys. Rev. Lett. **79**, 986 (1997).
- [18] V. Barger and C. Kao, Phys. Rev. D **57**, 3131 (1998).
- [19] R. Barate et al., the ALEPH Collaboration, Eur. Phys. J. **C2** (1998) 417.
- [20] G. Abbiendi et al., the OPAL Collaboration, CERN-EP-98-136, (1998), e-Print Archive: hep-ex/980903.
- [21] R. Arnowitt and P. Nath, Phys. Lett. B **289**, 368 (1992); S.P. Martin and P. Ramond, Phys. Rev. D **48**, 5365 (1993).
- [22] R. Oishi and Y. Seiya, talk presented at the Joint Working Group Meeting of Physics at Run II–Workshop on Supersymmetry/Higgs, Fermi National Accelerator Laboratory, Batavia, Illinois, September 3, 1998.
- [23] H. Baer, C.-H. Chen, M. Drees, F. Paige and X. Tata, Phys. Rev. D **58**, 075008 (1998).
- [24] J.D. Wells, Mod. Phys. Lett. **A13**, 1923 (1998).
- [25] J. Lykken and K. Matchev, talk presented at the Summary Meeting of Physics at Run II–Workshop on Supersymmetry/Higgs, Fermi National Accelerator Laboratory, Batavia, Illinois, November 18-21, (1998).
- [26] M.S. Alam et al., the CLEO Collaboration, Phys. Rev. Lett. **74** (1995) 2885.
- [27] R. Barate et al., the ALEPH Collaboration, Phys. Lett. B **429** (1998) 169.
- [28] P. Nath and R. Arnowitt, Phys. Lett. **B336** (1994) 395; Phys. Rev. Lett. **74** (1995) 4592; Phys. Rev. **D54** (1996) 2374; F. Borzumati, M. Drees and M. Nojiri, Phys. Rev. **D51** (1995) 341; H. Baer and M. Brhlik, Phys. Rev. **D55** (1997) 3201; H. Baer, M. Brhlik, D. Castano and X. Tata, Phys. Rev. D **58**, 015007 (1998).
- [29] T. Kamon, presented at the SUSY 98 Conference, Oxford, England, July 1998.
- [30] J. Nachtman, presented at the the Joint CDF/D0 SUGRA Working Group Meeting

of Physics at RUN II–Workshop on Supersymmetry/Higgs, Fermi National Accelerator Laboratory, Batavia, Illinois, November 18, 1998.

- [31] T. Plehn, Hamburg University Doctoral thesis DESY-THESIS-1998-024 (1998), hep-ph/9809319; W. Beenakker, M. Kramer, T. Plehn and M. Spira, talk presented at Physics at Run II: Workshop on Supersymmetry/Higgs: Summary Meeting, Batavia, IL, November (1998), hep-ph/9810290.
- [32] J. Ohnemus, Phys. Rev. D **44**, 3477 (1991); Phys. Rev. D **50**, 1931 (1994).
- [33] I. Hinchliffe, F.E. Paige, M.D. Shapiro , J. Soderqvist, W. Yao, Phys. Rev. **D55** (1997) 5520; A. Bartl, et al., presented at 1996 DPF/DPB Summer Study on New Directions for High-Energy Physics (Snowmass 96), Snowmass, CO, 25 June - 12 July, 1996.
- [34] H. Baer, C.-H. Chen, M. Drees, F. Paige and X. Tata, Florida State University Report FSU-HEP-980730 (1998), e-Print Archive: hep-ph/9809223
- [35] H. Baer et al., in progress;

TABLES

TABLE I. The cross section of $p\bar{p} \rightarrow 3\ell + X$ in fb versus $\tan\beta$ for $m_{1/2} = 200$ GeV and $m_0 = 100$ GeV along with the trilepton cross sections of the backgrounds from WZ , $t\bar{t}$, and ZZ at the upgraded Tevatron with cuts on isolation, missing E_T and $M_{\ell+\ell^-}$: $E_T(\text{cone}) < 2$ GeV, $\cancel{E}_T > 25$ GeV, and $|M_{\ell\ell} - M_Z| > 10$ GeV as well as soft and hard cuts: (a) Soft Cuts: $p_T(\ell_1) > 11$ GeV, $p_T(\ell_2) > 7$ GeV, $p_T(\ell_3) > 5$ GeV, $|\eta(\ell_1, \ell_2, \ell_3)| < 2.0$, and at least one lepton with $p_T(\ell) > 11$ GeV and $|\eta(\ell)| < 1.0$; (b) Soft Cuts and Jet-Veto(JV): we veto events with any jet that has $E_T > 15$ GeV; (c) Hard Cuts: $p_T(\ell_1) > 20$ GeV, $p_T(\ell_2) > 15$ GeV, $p_T(\ell_3) > 10$ GeV, $|\eta(\ell_1, \ell_2, \ell_3)| < 2.5$; (d) Hard Cuts and Jet-Veto (JV).

Case \ $\tan\beta$	3	10	20	25	WZ	$t\bar{t}$	ZZ
(a) Soft Cuts	13.5	3.62	1.17	0.73	0.40	0.14	0.04
(b) Soft Cuts +JV	7.3	1.74	0.44	0.29	0.24	0.002	0.01
(c) Hard Cuts	6.2	1.51	0.41	0.27	0.28	0.02	0.02
(d) Hard Cuts +JV	3.2	0.66	0.16	0.11	0.17	0.001	0.003

TABLE II. The cross section of $p\bar{p} \rightarrow 3\ell + X$ in fb versus $\tan\beta$ with contributions from various relevant SUSY channels at $\sqrt{s} = 2$ TeV with the acceptance cuts described in Eq. 5, for $\mu > 0$, $m_{1/2} = 200$ GeV, $\tan\beta = 2, 10, 20$ and 35 (25 for $m_0 = 100$ GeV).

Channel \ $\tan\beta$	2	10	20	35(25)
(i) $m_0 = 100$ GeV				
Total	14.30	3.62	1.17	0.73
$\chi_{\Gamma}^{\pm}\chi_2^0$	11.87	2.42	0.54	0.20
$\tilde{\ell}\tilde{\nu}$	0.96	0.47	0.23	0.16
$\tilde{\ell}\tilde{\ell}$	0.49	0.23	0.16	0.18
$\chi_2^0\chi_2^0, \chi_2^0\chi_3^0, \chi_3^0\chi_4^0,$	0.42	0.20	0.10	0.06
$\chi_{\Gamma}^{\pm}\chi_{3,4}^0, \chi_2^{\pm}\chi_{3,4}^0, \chi_{\Gamma}^{\pm}\chi_2^{\mp}, \chi_2^{\pm}\chi_2^{\mp}$	0.05	0.10	0.06	0.07
$\tilde{g}\chi_{2,3}^0, \tilde{q}\chi_{2,3}^0, \tilde{g}\tilde{g}, \tilde{q}\tilde{q}, \tilde{\nu}\tilde{\nu}$	0.51	0.20	0.08	0.06
(ii) $m_0 = 200$ GeV				
Total	3.34	0.35	0.29	0.40
$\chi_{\Gamma}^{\pm}\chi_2^0$	3.09	0.26	0.19	0.24
$\tilde{\ell}\tilde{\nu}$	0.12	0.03	0.04	0.04
$\tilde{\ell}\tilde{\ell}$	0.02	0.01	0.01	0.01
$\chi_2^0\chi_2^0, \chi_2^0\chi_3^0, \chi_3^0\chi_4^0,$	0.02	0.02	0.01	0.03
$\chi_{\Gamma}^{\pm}\chi_{3,4}^0, \chi_2^{\pm}\chi_{3,4}^0, \chi_{\Gamma}^{\pm}\chi_2^{\mp}, \chi_2^{\pm}\chi_2^{\mp}$	0.01	0.01	0.02	0.03
$\tilde{g}\chi_{2,3}^0, \tilde{q}\chi_{2,3}^0, \tilde{g}\tilde{g}, \tilde{q}\tilde{q}, \tilde{\nu}\tilde{\nu}$	0.08	0.02	0.02	0.05
(iii) $m_0 = 500$ GeV				
Total	0.46	0.62	0.68	0.69
$\chi_{\Gamma}^{\pm}\chi_2^0$	0.46	0.57	0.67	0.66
$\chi_2^0\chi_2^0, \chi_2^0\chi_3^0, \chi_3^0\chi_4^0,$	–	0.01	–	0.01
$\chi_{\Gamma}^{\pm}\chi_{3,4}^0, \chi_2^{\pm}\chi_{3,4}^0, \chi_{\Gamma}^{\pm}\chi_2^{\mp}, \chi_2^{\pm}\chi_2^{\mp}$	–	0.03	0.01	0.01
$\tilde{g}\chi_{2,3}^0, \tilde{q}\chi_{2,3}^0, \tilde{g}\tilde{g}, \tilde{q}\tilde{q}, \tilde{\nu}\tilde{\nu}$	–	0.01	–	0.01

TABLE III. The cross section (in fb) of $p\bar{p} \rightarrow 3\ell + X$ at $\sqrt{s} = 2$ TeV versus $\tan\beta$ with the acceptance cuts described in Eq. 5 and contributions from various SUSY channels for $\mu < 0$, $m_{1/2} = 160$ GeV, $\tan\beta = 2$ and several choices of m_0 .

Channel \ m_0 (GeV)	100	200	500	1000
Total	7.00	4.86	1.68	1.20
$\chi_1^\pm \chi_2^0$	5.55	4.03	1.64	1.18
$\tilde{\ell}\tilde{\nu}$	0.11	0.11	–	–
$\tilde{\ell}\tilde{\ell}$	0.12	0.05	–	–
$\chi_2^0\chi_2^0, \chi_2^0\chi_3^0, \chi_3^0\chi_4^0,$	0.20	0.14	0.01	–
$\chi_1^\pm\chi_{3,4}^0, \chi_2^\pm\chi_{3,4}^0, \chi_1^\pm\chi_2^\mp, \chi_2^\pm\chi_2^\mp$	0.08	0.03	0.08	–
$\tilde{g}\chi_{2,3}^0, \tilde{q}\chi_{2,3}^0, \tilde{g}\tilde{g}, \tilde{q}\tilde{q}, \tilde{\nu}\tilde{\nu}$	0.94	0.49	0.03	0.02

TABLE IV. The cross section of $p\bar{p} \rightarrow \chi_2^0\chi_2^0 \rightarrow 4\ell + X$ in fb versus $\tan\beta$ for $m_{1/2} = 200$ GeV and $m_0 = 100$ GeV along with the 4-lepton cross section of the background from WZ and ZZ , at the upgraded Tevatron with soft cuts: $E_T(\text{cone}) < 2$ GeV, $p_T(\ell_1) > 11$ GeV, $p_T(\ell_2) > 7$ GeV, $p_T(\ell_3, \ell_4) > 5$ GeV, $|\eta(\ell)| < 2.0$, at least one lepton with $p_T(\ell) > 11$ GeV, and $|\eta(\ell)| < 1.0$.

Case \ $\tan\beta$	3	10	20	25	ZZ
Soft Cuts	0.79	0.21	0.11	0.08	0.17

FIGURES

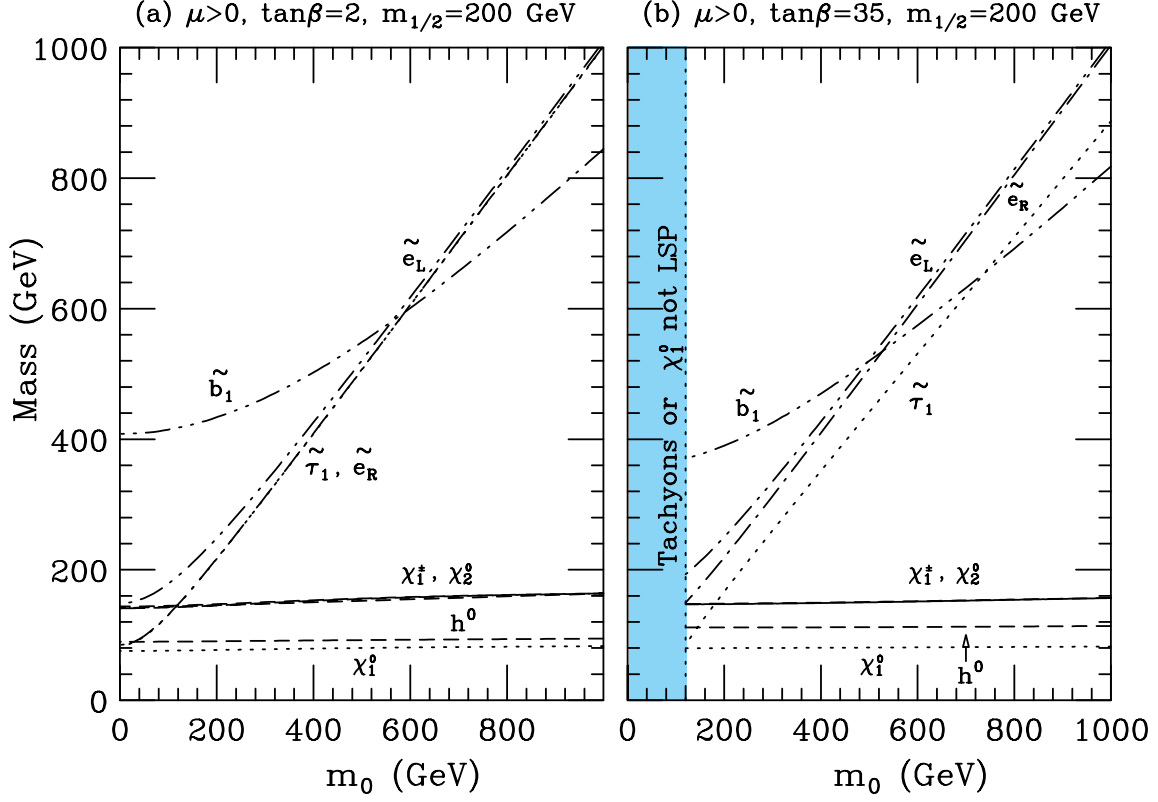


FIG. 1. Masses of χ_1^0 , χ_2^0 , χ_1^\pm , \tilde{e}_L , \tilde{e}_R , $\tilde{\tau}_1$ and \tilde{b}_1 at the M_Z mass scale and mass of h^0 at the mass scale $Q = \sqrt{m_{\tilde{l}_L} m_{\tilde{l}_R}}$, versus m_0 , with $M_{\text{SUSY}} = 1$ TeV, $m_{1/2} = 200$ GeV and $\mu > 0$ for (a) $\tan\beta = 2$ and (b) $\tan\beta = 35$. The shaded regions are excluded by theoretical requirements (EWSB, tachyons, LSP),

$$q\bar{q}' \rightarrow \chi_1^\pm \chi_2^0$$

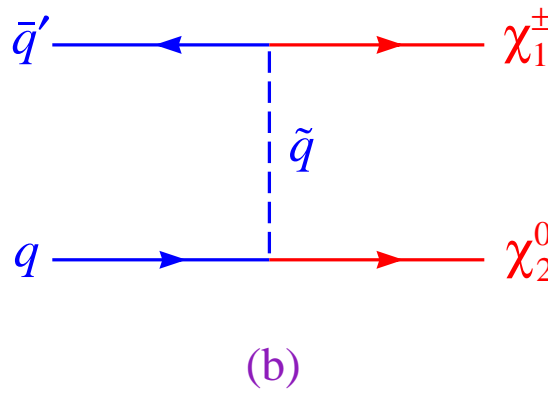
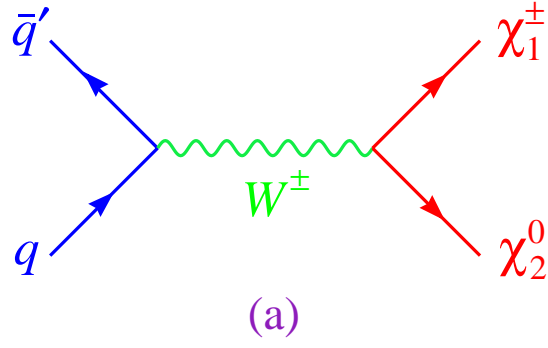


FIG. 2. Feynman diagrams of $q\bar{q}' \rightarrow \chi^\pm \chi_2^0$.

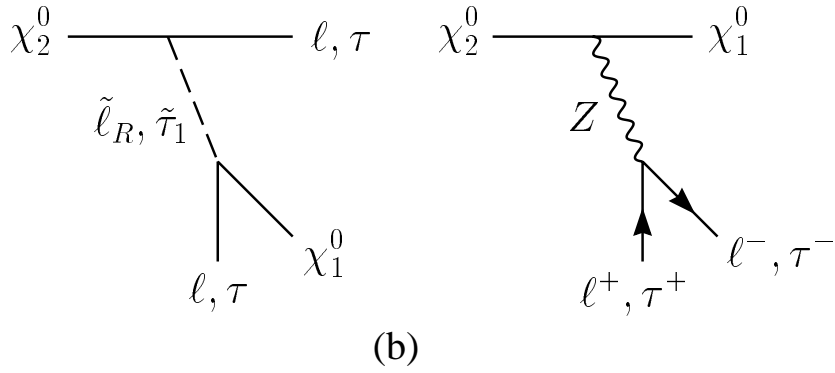
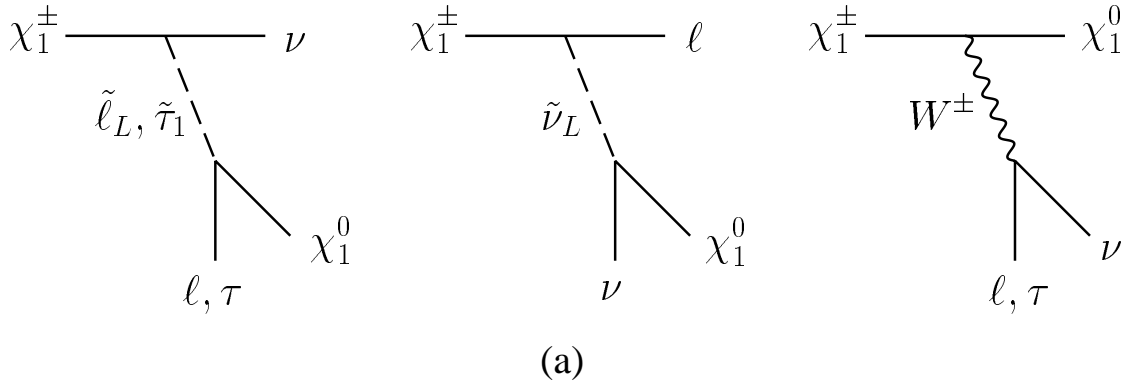


FIG. 3. Feynman diagrams of (a) $\chi_1^\pm \rightarrow l\nu\chi_1^0$ or $\tau\nu\chi_1^0$ and (b) $\chi_2^0 \rightarrow l^+l^-\chi_1^0$ or $\tau^+\tau^-\chi_1^0$.

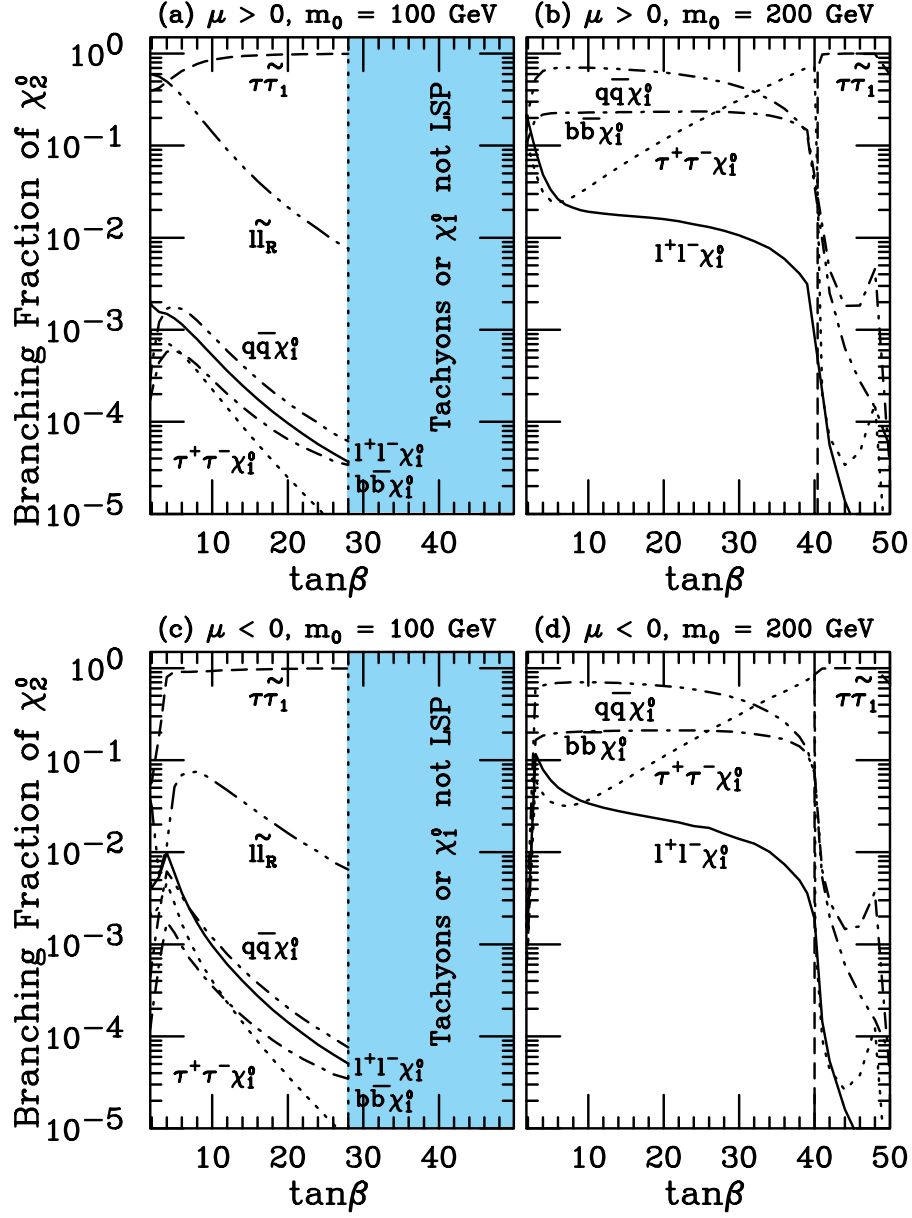


FIG. 4. Branching fractions of χ_2^0 decays into various channels versus $\tan\beta$ with $m_{1/2} = 200$ GeV, for (a) $\mu > 0$ and $m_0 = 100$ GeV, (b) $\mu > 0$ and $m_0 = 200$ GeV, (c) $\mu < 0$ and $m_0 = 100$ GeV, and (d) $\mu < 0$ and $m_0 = 200$ GeV.

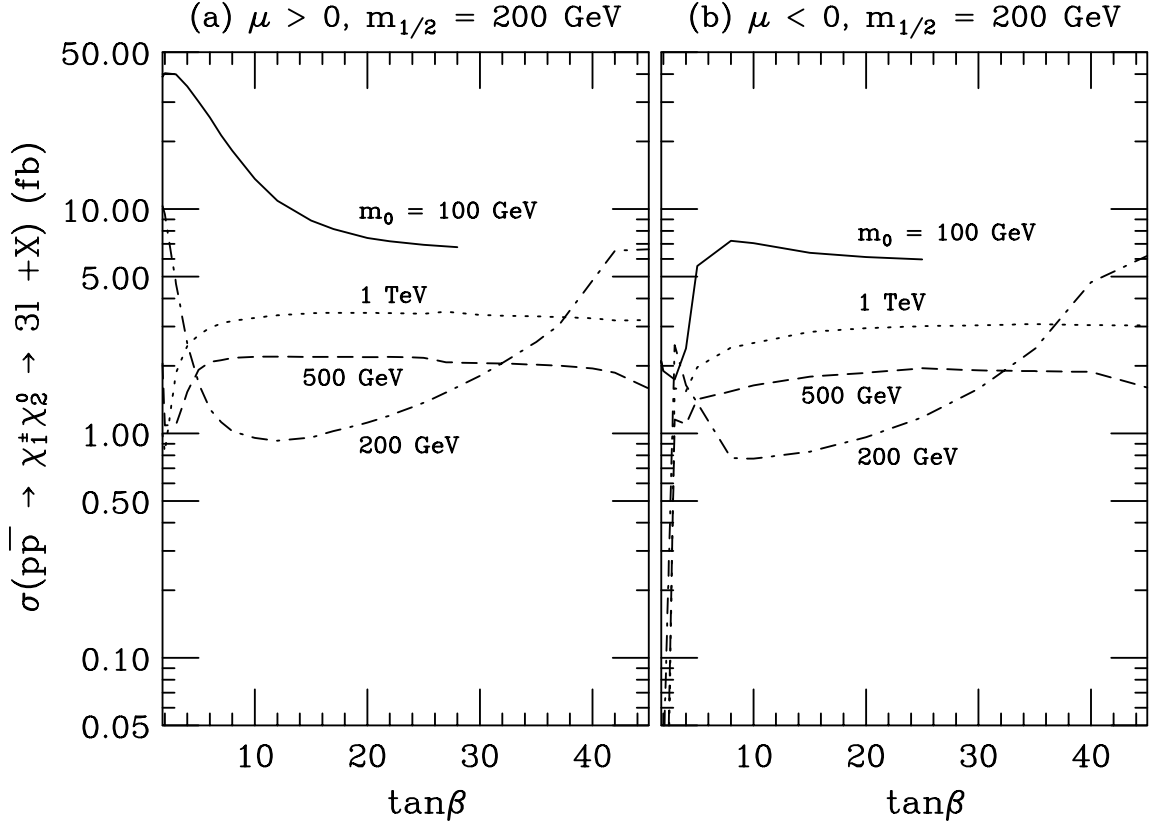


FIG. 5. Cross section of $p\bar{p} \rightarrow \chi_1^\pm \chi_2^0 \rightarrow 3\ell + X$ at $\sqrt{s} = 2 \text{ TeV}$ without cuts versus $\tan\beta$, with $m_{1/2} = 200 \text{ GeV}$ and several values of m_0 for (a) $\mu > 0$ and (b) $\mu < 0$.

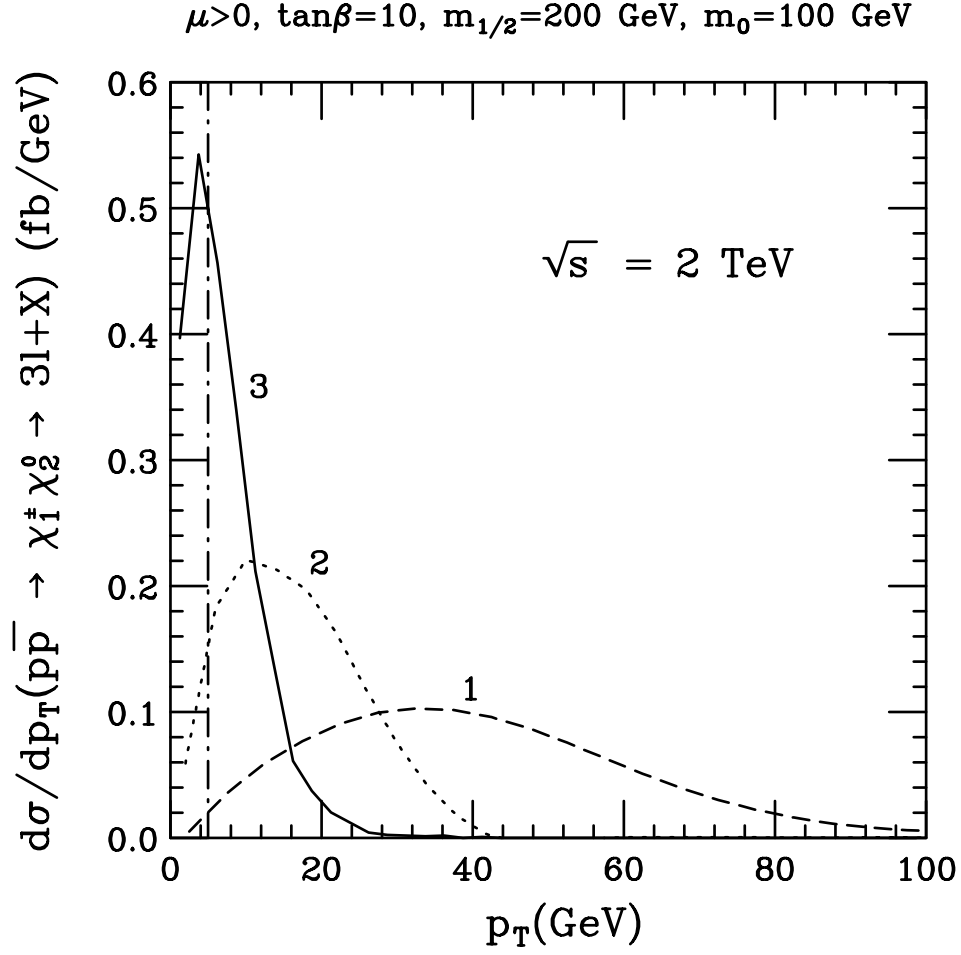


FIG. 6. Transverse momentum (p_T) distribution of $p\bar{p} \rightarrow \chi_1^\pm \chi_2^0 \rightarrow 3\ell + X$ at $\sqrt{s} = 2 \text{ TeV}$ with $\mu > 0$, $\tan\beta = 3$, $m_{1/2} = 200 \text{ GeV}$ and $m_0 = 100 \text{ GeV}$, for the three leptons with $p_T(\ell_1) > p_T(\ell_2) > p_T(\ell_3)$.

$$W^\pm Z \rightarrow 3l + X \text{ via } Z \rightarrow \tau^+ \tau^-$$

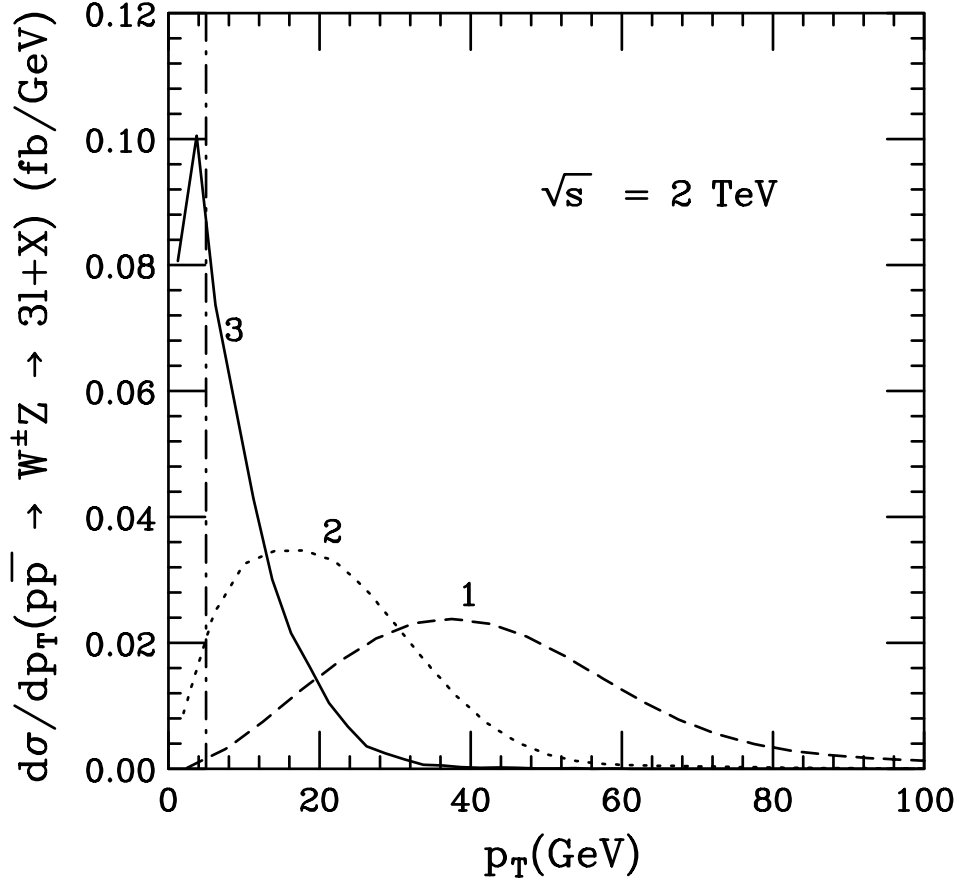


FIG. 7. Transverse momentum (p_T) distribution of the dominant background from the associated WZ production, $p\bar{p} \rightarrow W^\pm Z \rightarrow 3l + X$, via $Z \rightarrow \tau^+ \tau^- \rightarrow l^+ l^- + X$, at $\sqrt{s} = 2 \text{ TeV}$, for the three leptons with $p_T(\ell_1) > p_T(\ell_2) > p_T(\ell_3)$.

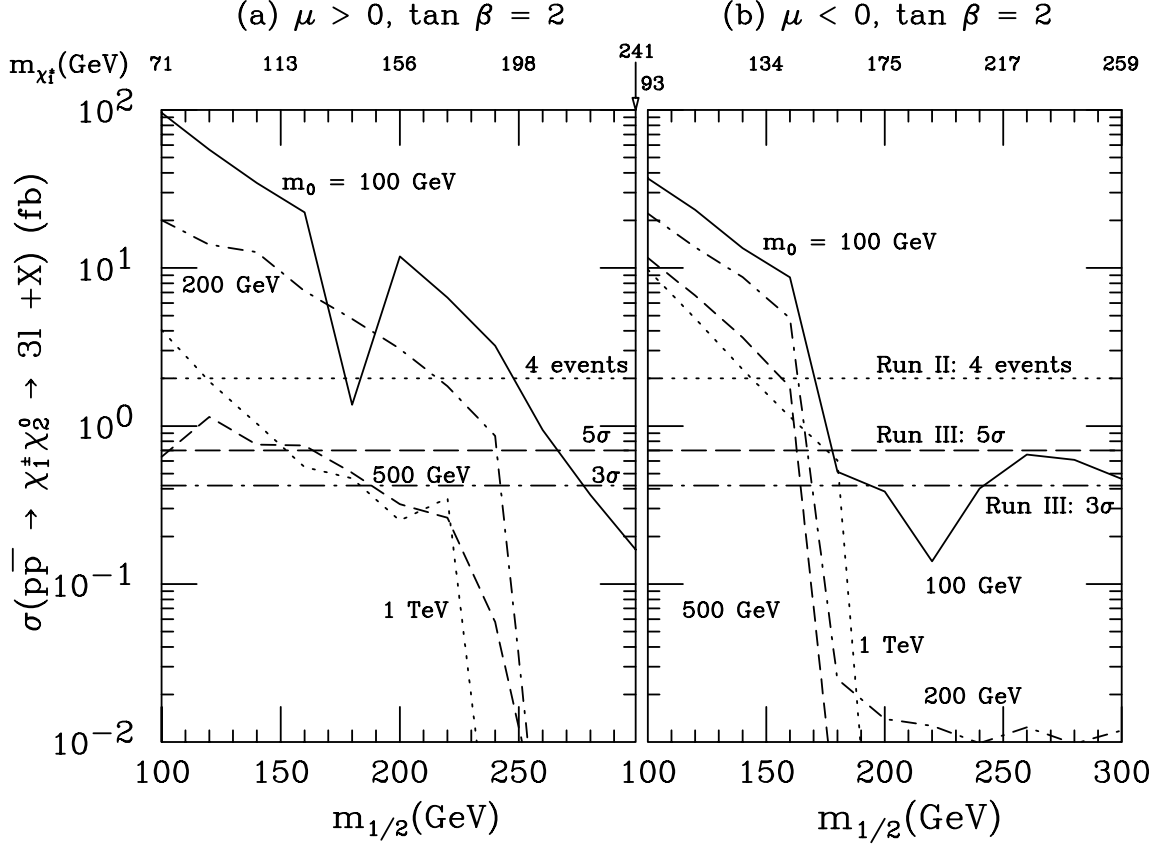


FIG. 8. Cross section of $p\bar{p} \rightarrow \chi_1^\pm \chi_2^0 \rightarrow 3\ell + X$ at $\sqrt{s} = 2$ TeV, with soft acceptance cuts (Eq. 5), versus $m_{1/2}$, with $\tan\beta = 2$, $m_0 = 100$ GeV (solid), 200 GeV (dot-dash), 500 GeV (dash) and 1000 GeV (dot). for (a) $\mu > 0$ and (b) $\mu < 0$, Also noted are the cross sections for (i) 4 signal events with $L = 2 \text{ fb}^{-1}$ (dot), (ii) 5σ signal for $L = 8 \text{ fb}^{-1}$ (dash) and (iii) 5σ signal for $L = 30 \text{ fb}^{-1}$ (dot-dash). The chargino mass evaluated with $m_0 = 500$ GeV is presented as well.

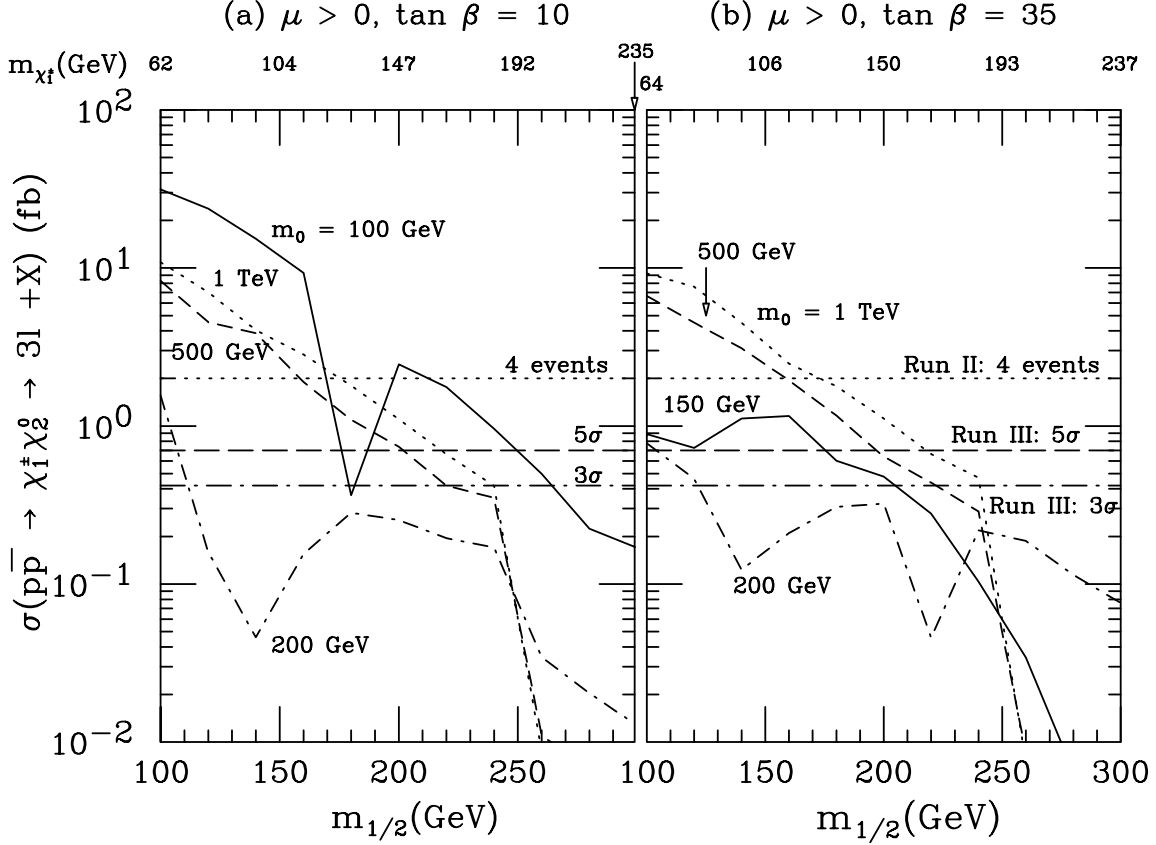


FIG. 9. Cross section of $p\bar{p} \rightarrow \chi_1^\pm \chi_2^0 \rightarrow 3\ell + X$ at $\sqrt{s} = 2$ TeV, with soft acceptance cuts (Eq. 5), versus $m_{1/2}$, with $\mu > 0$, $m_0 = 100$ GeV (solid), 200 GeV (dot-dash), 500 GeV (dash) and 1000 GeV (dot), for (a) $\tan \beta = 10$ and (b) $\tan \beta = 35$. Also noted are the cross sections for (i) 4 signal events with $L = 2 \text{ fb}^{-1}$ (dot), (ii) 5σ signal for $L = 8 \text{ fb}^{-1}$ (dash) and (iii) 5σ signal for $L = 30 \text{ fb}^{-1}$ (dot-dash). The chargino mass evaluated with $m_0 = 500$ GeV is presented as well.

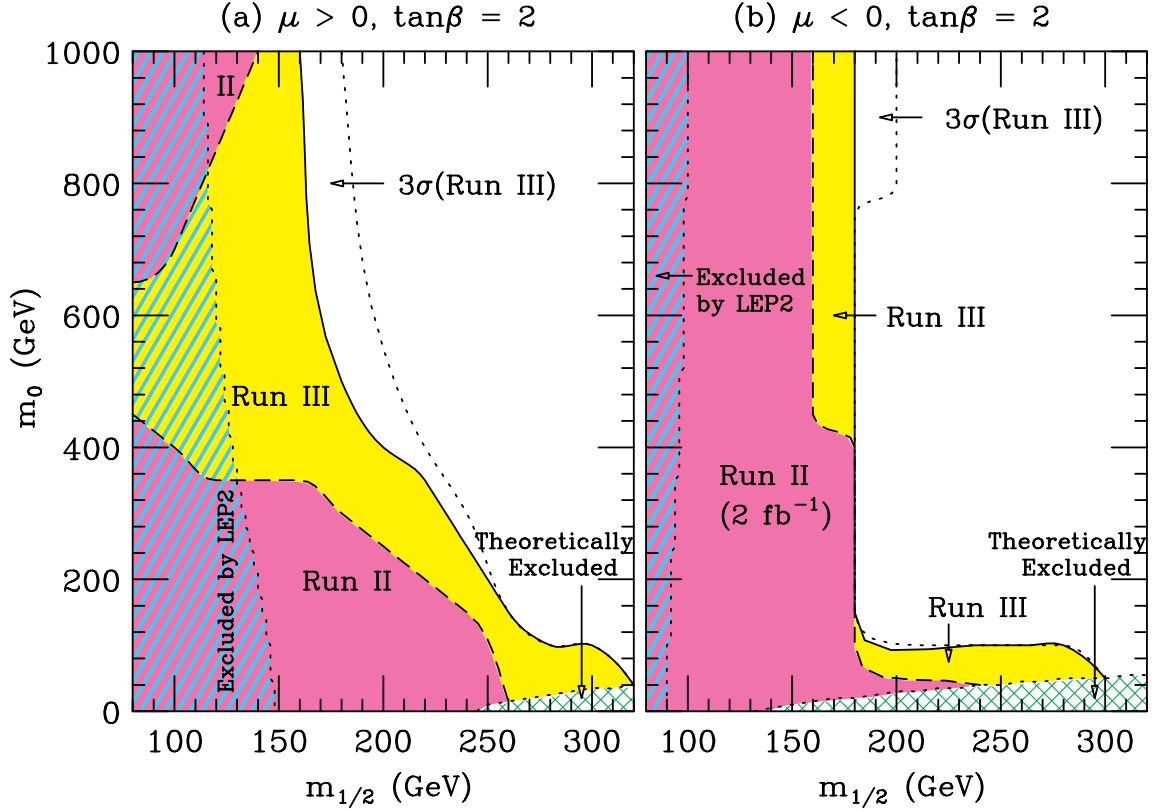


FIG. 10. Discovery contours at 99% C.L. (Run II) and 5σ (Run III) for $p\bar{p} \rightarrow \chi_1^\pm \chi_2^0 \rightarrow 3\ell + X$ at $\sqrt{s} = 2$ TeV, with soft acceptance cuts (Eq. 5), in the parameter space of $(m_{1/2}, m_0)$, with $\tan\beta = 2$, for (a) $\mu > 0$ and (b) $\mu < 0$. All SUSY sources of trileptons are included. The shaded regions denote the parts of the parameter space (i) excluded by theoretical requirements, or (ii) excluded by the chargino search at LEP 2.

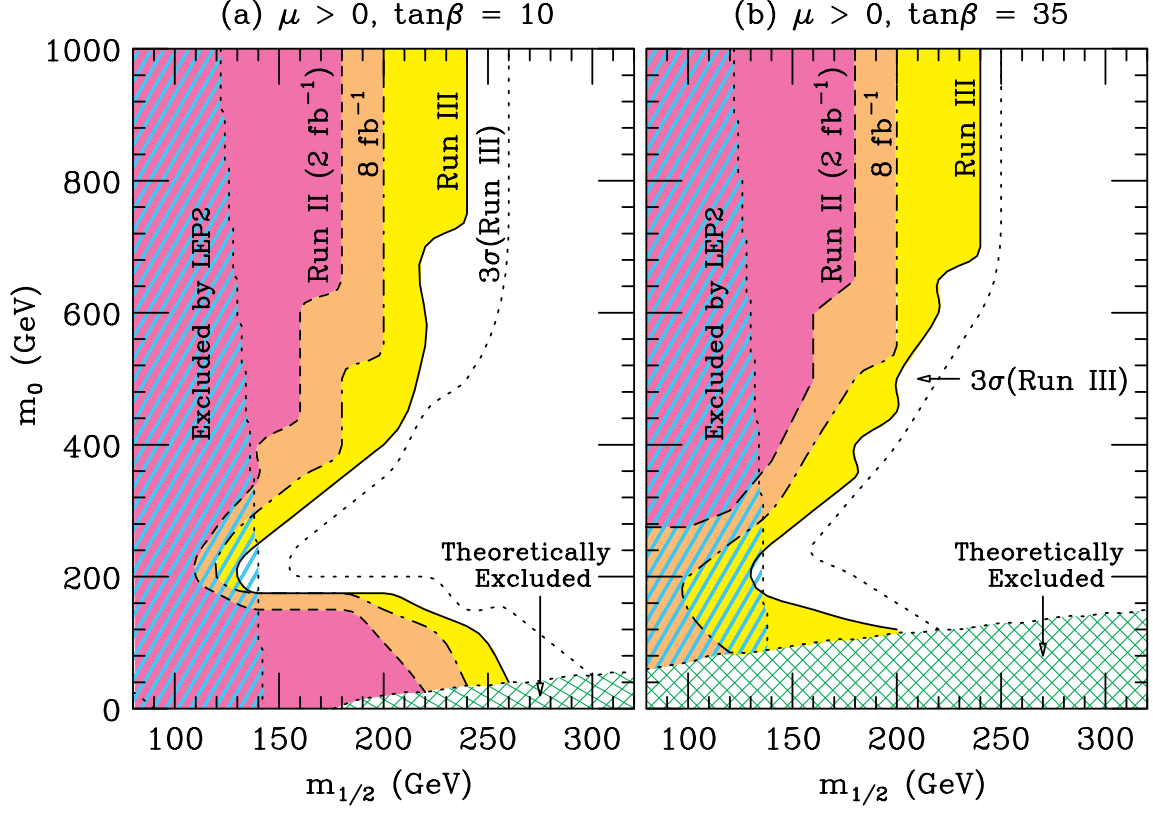


FIG. 11. Discovery contours at 99% C.L. (Run II) and 5σ (Run III) for $p\bar{p} \rightarrow 3\ell + X$ at $\sqrt{s} = 2$ TeV, with soft acceptance cuts (Eq. 5), in the parameter space of $(m_{1/2}, m_0)$, with $\mu > 0$, for (a) $\tan\beta = 10$ and (b) $\tan\beta = 35$. All SUSY sources of trileptons are included. The shaded regions denote the parts of the parameter space (i) excluded by theoretical requirements, or (ii) excluded by the chargino search at LEP 2.

$$\sqrt{s} = 2 \text{ TeV}, \mu > 0, \tan\beta = 3$$

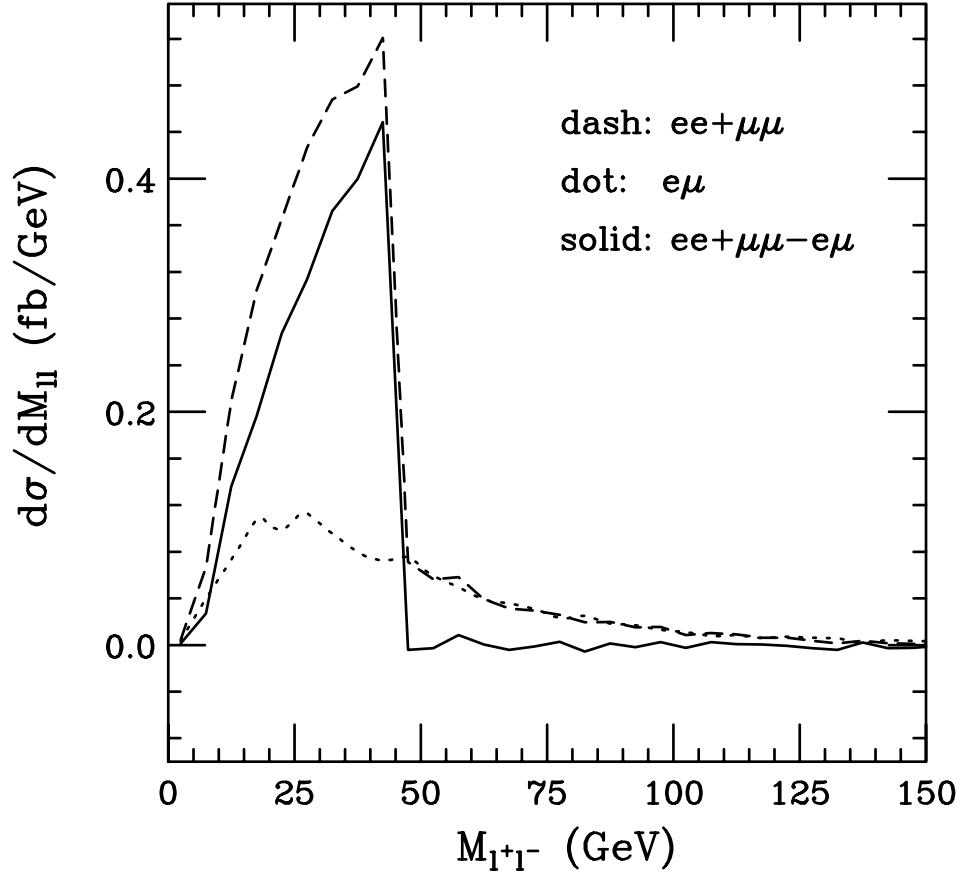


FIG. 12. The subtracted invariant mass distribution for two leptons with opposite signs (l^+l^-) as defined in Eq. 6, for $p\bar{p} \rightarrow \chi_1^\pm \chi_2^0 \rightarrow 3l + X$ at $\sqrt{s} = 2$ TeV, with $\mu > 0$, $\tan\beta = 3$, $m_{1/2} = 200$ GeV, and $m_0 = 100$ GeV.